

Seasonal influence of freshwater discharge on spatio-temporal variations in primary productivity, sea surface temperature, and euphotic zone depth in the northern Bay of Bengal

Hafez Ahmad^{1,2,3}, Felix Jose^{3*}, Md. Simul Bhuyan^{4,5}, Md. Nazrul Islam⁶, Padmanava Dash⁷

¹ Geosystems Research Institute/Department of Geosciences, Mississippi State University, Starkville 39759, USA

² Department of Oceanography, University of Chittagong, Chittagong 4331, Bangladesh

³ Department of Marine & Earth Sciences, Florida Gulf Coast University, Fort Myers 33965, USA

⁴ Bangladesh Oceanographic Research Institute, Cox's Bazar 4730, Bangladesh

⁵ Faculty of Marine Sciences & Fisheries, Institute of Marine Sciences, University of Chittagong, Chittagong 4331, Bangladesh

⁶ Department of Geography and Environment, Jahangirnagar University, Dhaka 1342, Bangladesh

⁷ Department of Geosciences, Mississippi State University, Starkville 39759, USA

Received 16 May 2023; accepted 11 September 2023

© Chinese Society for Oceanography and Springer-Verlag GmbH Germany, part of Springer Nature 2024

Abstract

Ocean productivity is the foundation of marine food web, which continuously removes atmospheric carbon dioxide and supports life at sea and on land. Spatio-temporal variability of net primary productivity (NPP), sea surface temperature (SST), sea surface salinity (SSS), mixed layer depth (MLD), and euphotic zone depth (EZD) in the northern Bay of Bengal (BoB) during three monsoon seasons were examined in this study based on remote sensing data for the period 2005 to 2020. To compare the NPP distribution between the coastal zones and open BoB, the study area was divided into five zones (Z1–Z5). Results suggest that most productive zones Z2 and Z1 are located at the head bay area and are directly influenced by freshwater discharge together with riverine sediment and nutrient loads. Across Z1–Z5, the NPP ranges from 5 315.38 mg/(m²·d) to 346.7 mg/(m²·d) (carbon, since then the same). The highest monthly average NPP of 5 315.38 mg/(m²·d) in February and 5 039.36 mg/(m²·d) in June were observed from Z2, while the lowest monthly average of 346.72 mg/(m²·d) was observed in March from Z4, which is an oceanic zone. EZD values vary from 6–154 m for the study area, and it has an inverse correlation with NPP concentration. EZD is deeper during the summer season and shallower during the wintertime, with a corresponding increase in productivity. Throughout the year, monthly SST shows slight fluctuation for the entire study area, and statistical analysis shows a significant correlation among NPP, and EZD, overall positive between NPP and MLD, whereas no significant correlation among SSS, and SST for the northern BoB. Long-term trends in SST and productivity were significantly positive in head bay zones but negatively productive in the open ocean. The findings in this study on the distribution of NPP, SST, SSS, MLD, and EZD and their seasonal variability in five different zones of BoB can be used to further improve the management of marine resources and overall environmental condition in response to climate changes in BoB as they are of utmost relevance to the fisheries for the three bordering countries.

Key words: chlorophyll *a*, sea surface temperature, euphotic zone depth, primary productivity, Ganges-Brahmaputra, ocean color, Bay of Bengal, monsoon

Citation: Ahmad Hafez, Jose Felix, Bhuyan Md. Simul, Islam Md. Nazrul, Dash Padmanava. 2024. Seasonal influence of freshwater discharge on spatio-temporal variations in primary productivity, sea surface temperature, and euphotic zone depth in the northern Bay of Bengal. *Acta Oceanologica Sinica*, 43(6): 1–14, doi: 10.1007/s13131-023-2254-y

1 Introduction

Ocean color (OC) is an important proxy for studying primary productivity in oceans, as it is measured by satellite sensors through the interaction of incident light with optically active substances present in the upper water column up to the euphotic zone depth (EZD). These optically active substances include suspended sediments, colored dissolved organic matter (CDOM), and chlorophyll *a* (Chl *a*) (Frolov et al., 2012). Water leaving radiance measured at the visible portion of the electromagnetic spectrum measures the presence of these optically active substances on the ocean surface. The net primary productivity (NPP), on the

other hand, measures how much inorganic carbon is fixed by phytoplankton per unit volume of water per unit of time (Sakalli, 2017). In addition to NPP, other biophysical parameters such as sea surface temperature (SST), EZD, mixed layer depth (MLD), CDOM, nitrate, phosphate, and sea surface salinity (SSS) play a crucial role in regulating phytoplankton biomass, ocean productivity, and community structure. Therefore, a better understanding of these parameters is essential for studying marine ecosystems and their response to various environmental factors (Mutshinda et al., 2013). The ocean primary productivity, which is the base of ocean food web and a key process for fixing energy

Foundation item: The US Department of State for sponsoring undergraduate exchange program.

*Corresponding author, E-mail: fjose@fgcu.edu

within the ecosystem, is directly influenced by these parameters. It removes atmospheric carbon dioxide and supports life on land and in the oceans (Arthur et al., 1987; Balch et al., 1992; Frey et al., 2017). Primary productivity also influences planktivorous and predatory organisms, mammals, and seabirds via zooplankton dynamics (Capuzzo et al., 2018; Hossain et al., 2020; Raymont, 2014), and plays a major role in ocean biogeochemical, ecological, and biological processes (Mohanty et al., 2014; Sarker and Wiltshire, 2017). Moreover, marine phytoplankton fixes 30–50 billion tons of carbon annually, equivalent to 40%–50% of the global total, via this process (Raymont, 2014). Observing interannual or long-term productivity variations provides insight into how changes in the ocean environment propagate from primary producers to higher trophic levels (Salgado-Hernanz et al., 2019). The productivity variations are determined by phytoplankton concentration together with photosynthetically available radiation (PAR) and SST in the EZD since phytoplankton blooms depend on the availability of sunlight, nutrients, and mechanisms that regulate them seasonally (Behrenfeld and Falkowski, 1997). Coastal and estuarine ecosystems exhibit maximum temporal and spatial variability in productivity due to variability in biological, biochemical, and physical properties of coastal waters, such as monsoonal wind circulation, river fluxes, coastal ocean circulation, upwelling, rainfall, and open ocean vertical stratification (Abdul-Hadi et al., 2013; Hendiarti et al., 2004; Satpathy et al., 2011). The Bay of Bengal (BoB) is an important region located to the east of the Indian subcontinent, receiving freshwater input from several major rivers such as the Ganges, Brahmaputra, Meghna, Krishna, Godavari, Mahanadi, Sittang, Irrawaddy, and Salween. Despite its significance, the BoB is known to be less productive compared to the Arabian Sea, located to the west of India. This could be attributed to the inability of the monsoon winds to break the upper-ocean stratification caused by high freshwater input from rivers and the torrential rainfall in the BoB. These conditions inhibit the mixing of water layers and consequently reduce the availability of nutrients, which are crucial for primary productivity (Saikranthi et al., 2019). In addition, the limited penetration of sunlight due to intense cloud cover and the persistent presence of turbid coastal waters, extending offshore as mud plumes, also play a significant role in inhibiting sustained high productivity in the northern BoB (Bharathi et al., 2018).

The BoB is both environmentally and economically an important region, as millions of people rely on this regional sea for their livelihood. Marine and estuarine fisheries play a crucial role in terms of livelihood, food sources, and supporting the national economy of the bordering countries (Hussain and Hoq, 2010; Shamsuzzaman et al., 2017). The abundance and distribution of fisheries depend heavily on the seasonal primary productivity of the Bay. A few studies reported the BoB's seasonal productivity and SST distribution with different approaches and for different periods (Mahesh et al., 2020; Pramanik et al., 2019; Zhou et al., 2020). Hence, this study aims to investigate the relationship between biophysical parameters such as NPP, SST, EZD, SST, and SSS in regulating phytoplankton biomass, ocean productivity, and community structure in the BoB. The study also aims to examine the interannual or long-term productivity variations to gain insight into how changes in the ocean environment propagate from primary producers to higher trophic levels. Specifically, the study will focus on determining the relationship between physical parameters and NPP and how this relationship is affected by varying SSS and SST in the BoB. Additionally, the study will explore the impact of wind reversal to flux on these relation-

ships, building on previous research. Overall, this research aims to contribute to a better understanding of the complex interactions between biophysical parameters and their impact on ocean productivity and ecosystem dynamics in the BoB.

2 Materials and methods

2.1 Study area

The study area covers the northern BoB between 17°N to 23°N latitudes and 85°E to 95°E longitudes. The BoB is situated on the eastern side of the Indian subcontinent (Fig. 1), surrounded by land except for the south, where it is exposed to the influence of the open Indian Ocean. For ease of comparing NPP, MLD, SST, SSS, and EZD variability, the study area has been divided into five rectangular zones: Z1, Z2, Z3, Z4, and Z5. This division is based on relative river influence, currents in the bay, and coastal geography. Z1 is dominated by the influence of mangrove forests (Sundarbans) and riverine freshwater input (Hooghly Estuary), whereas Z2 is dominated by freshwater discharge from the Ganges, the Brahmaputra, Karnaphuli, and Meghna river systems and the persistence of high turbidity. Z4 is entirely in the open ocean, significantly away from any river influence, and is subjected to stratification, which influences primary productivity. Z3 is the southwestern part of the BoB, where the circulation dynamics are influenced by the seasonally reversing East Indian equatorial current, and the major influencing rivers are Brahmani, Mahanadi, and Godavari rivers. In contrast, Z5, along the Myanmar-Bangladesh coast, exhibits relatively stable coastal upwelling and circulation dynamics, and the major influencing rivers are the Irrawaddy and Kaladan Rivers.

We downloaded monthly gridded satellite images of ocean color and sea surface temperature, along with analyzed gridded data on NPP, from Aqua MODIS archives (<https://coastwatch.pfeg.noaa.gov>), MLD from https://archive.podaac.earthdata.nasa.gov/podaac-ops-cumulus-protected/ECCO_L4_MIXED_LAYER_DEPTH_05DEG_MONTHLY_V4R4 and EZD (<https://giovanni.gsfc.nasa.gov>), respectively. The data were obtained for the BoB study area, which is located between 16°N to 22.5°N and 79°E to 95°E, covering the period of 2005 to 2020. SSS data for 2015–2020 was downloaded from the physical oceanography distributed active archive center (https://podaac.jpl.nasa.gov/dataset/SMAP_RSS_L3_SSS_SMI_MONTHLY_V4) and for the period 2010–2015, monthly surface salinity gridded data product v1.8 were retrieved from the European Space Agency Climate Change Initiative (http://data.ceda.ac.uk/neodc/esacci/sea_surface_salinity). Based on the data from the dates for which salinity data were available from both sources, two datasets were converted into the same unit. At first, the Shapiro normality test was used; both datasets are normality distributed (ESA: $p = 0.186$, and smap: $p = 0.292$). Then, the F -test ($p = 0.315$), which means the variance of the two datasets is equal, and after that, we conducted a T -test ($p = 0.562$), which indicates means were also equal. Subsequently, datasets were merged. These data were extracted from the five zones and analyzed for their monthly and inter-annual variability in SST, NPP, SSS, EZD, and MLD. These data were resampled seasonally for the southwest monsoon (SW monsoon) (average of data from June to September), northeast monsoon (NE monsoon) (average of data from October to December), and pre-monsoon (average of data from March to May) and plotted for the six years using Python's Xarray library (Hoyer and Hamman, 2017).

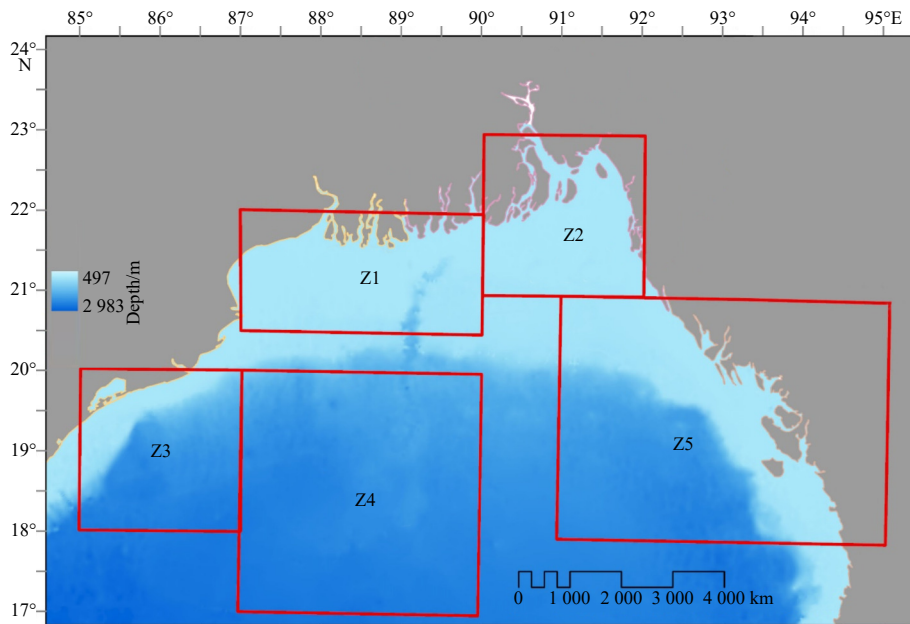


Fig. 1. Map of the Bay of Bengal and the five zones (Z1–Z5) identified for studying the NPP, SST, SSS, MLD, and EZD variability (coastline data retrieved from <https://www.naturalearthdata.com> and Bathymetric data from <https://www.gebco.net>).

2.2 Wind pattern in the northern BoB

Circulation dynamics and marine productivity in the northern BoB are controlled by the seasonally reversing wind system called the monsoon. The pre-monsoon season occurs from March to May and is followed by the summer monsoon or SW monsoon, which dominates the Indian sub-continent from June to September (Fig. 2). NE monsoon occurs from October to December, also called Post-monsoon (Prakash and Pant, 2020). The post-monsoon wind system blows from land to sea, whereas the SW monsoon blows from sea to land (Vinayachandran and Kurian, 2007), and it brings a steady stream of moisture that triggers torrential rainy season in the region accompanied by mudslides and transport of heavy load of suspended sediment to the ocean. The SW monsoon contributes to 80% of the annual rainfall over the Indian subcontinent (Saikranthi et al., 2019). In addition, the Indian Ocean Dipole (IOD) impacts circulation in the BoB.

During summer, upwelling along the eastern Indian coast due to the SW monsoon increases productivity compared to the downwelling favorable NE monsoon wind system during winter (Thushara and Vinayachandran, 2016). The SST is generally lower during winter, and it remains higher during the rest of the year (28.5–29°C). Meridional variation of SST in the northern BoB is almost constant, and it varies between 28°C to 28.5°C, with the highest SST reported in the southwest part of BoB (Jaswal et al., 2012). Occasional passage of cyclones across the bay also contributes to the large-scale mixing of the water column and the infusion of nutrients into the photic zone (Prasanna Kumar et al., 2002). During the summer monsoon, salinity drops to ~1 in the head bay region, and it increases to 15–20 during winter (Rahman, 2007).

2.3 Hydrology and nutrient discharge

Freshwater influxes play a significant role in controlling ocean productivity. Surface currents distribute the freshwater along the coast and lower the salinity level, creating a barrier layer that impedes convection and limits vertical mixing and heat flow. Stratification restricts the movement of nutrients,

which reduces productivity (Narvekar and Prasanna Kumar, 2014; Kay et al., 2018). However, the degree of stratification is determined by freshwater input, monsoonal wind intensity, SST, water clarity, and ocean currents (Gopalakrishna et al., 2002). Head bay experiences the highest river discharge during SW monsoon when rainfall is generally at its peak, and it is minimal during the winter and pre-monsoon (Sandeep and Pant, 2019). During SW monsoon, the river influx doubled to nearly 183×10^{11} m³/s. The rivers of Bangladesh alone supply 1.222×10^6 m³/s of freshwater into the northern part of the bay (Sandeep and Pant, 2019). Monthly river discharge has the maximum between July and September when the region is exposed to strong and sustained wind from a southwesterly direction with high precipitation (Fig. 3).

3 Results

3.1 Monthly and seasonal spatio-temporal distribution of NPP

Across Z1–Z5, the NPP ranges from 5 315 mg/(m²·d) to 346.7 mg/(m²·d) (Fig. 4). Z2 had the highest NPP, while Z4 had the lowest. Compared with other zones, Z2 has the highest productivity, Z1 has the second-highest productivity, and Z4 has the least productivity. In almost all months, Z1 exhibits higher productivity, but August to November have NPPs greater than 3 273 mg/(m²·d). Z2 has relatively higher productivity in February, March, June, and August to October, with 4 336 mg/(m²·d) or more. Z3 and Z5 show moderate productivity compared to Z1 and Z2. Z3's monthly NPPs range from 4 719 mg/(m²·d) (April) to 462 mg/(m²·d) (March), while Z5's NPPs range from 1 434 mg/(m²·d) (February) to 576 mg/(m²·d) (November). Z4 shows low productivity and the least monthly variation in which NPP varies from 795 mg/(m²·d) (September) to 346 mg/(m²·d) (March) (Figs 4 and 5).

NPPs vary greatly from season to season; for example, in Z1, NPPs range from 2 915 mg/(m²·d) to 1 627 mg/(m²·d); NE monsoon shows higher, whereas pre-monsoon shows the lowest. However, the same seasonal variation is not happening in Z2, where the SW monsoon shows higher NPP (5 757 mg/(m²·d))

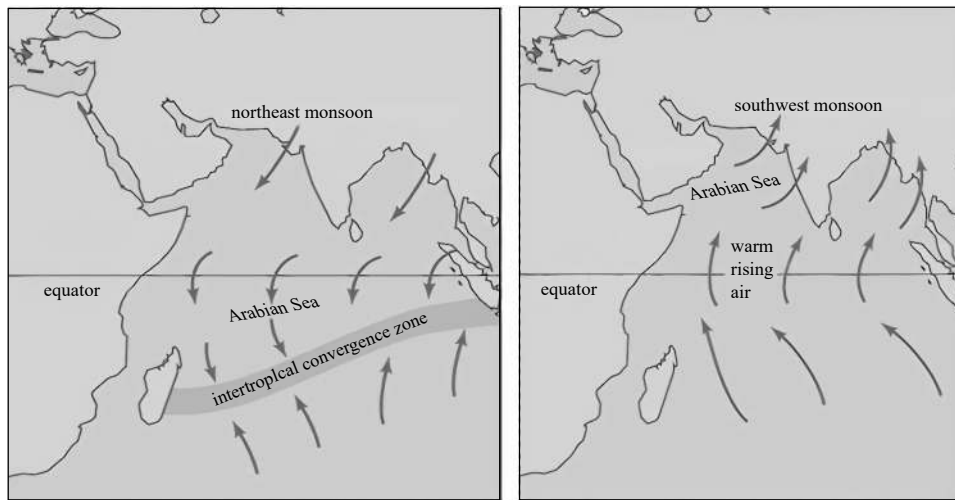


Fig. 2. Prevailing northeast and southwest monsoons in the Bay of Bengal and the Arabian Sea. The arrow indicates the direction of wind flow.

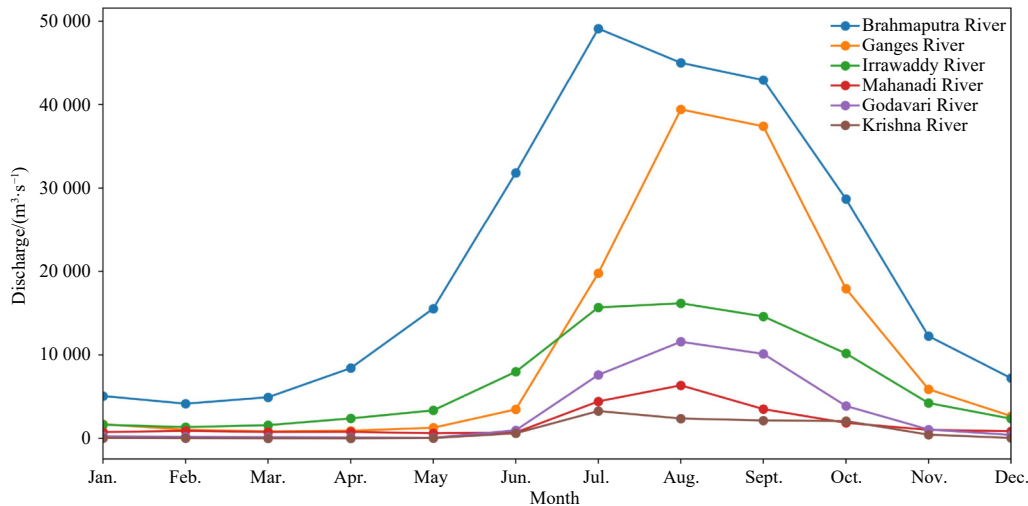


Fig. 3. Freshwater discharge (m^3/s) from the six major rivers flowing into the Bay of Bengal. Monthly discharge rates for the Brahmaputra River, Ganges River, Irrawaddy River, Mahanadi River, Godavari River, and Krishna River. Data was retrieved from the Global Runoff Data Centre at <https://portal.grdc.bafg.de/>.

and the NE monsoon shows lower ($4\,004\text{ mg}/(\text{m}^2\cdot\text{d})$). The exact opposite of Z2 is found in Z5, but the magnitude is comparatively lower in Z5; for instance, seasonal NPP varies from $1\,071\text{ mg}/(\text{m}^2\cdot\text{d})$ to $682\text{ mg}/(\text{m}^2\cdot\text{d})$. Interestingly, Z3 and Z4 have the exact opposite scenario to Z1, where NPPs range from $900\text{ mg}/(\text{m}^2\cdot\text{d})$ to $681\text{ mg}/(\text{m}^2\cdot\text{d})$ and $473\text{ mg}/(\text{m}^2\cdot\text{d})$ to $373\text{ mg}/(\text{m}^2\cdot\text{d})$, respectively (Fig. 6, Table 1).

As Z2 shows maximum productivity, this zone also shows the highest seasonal variability, ranging from $4\,049\text{ mg}/(\text{m}^2\cdot\text{d})$ (pre-monsoon) to $1\,582\text{ mg}/(\text{m}^2\cdot\text{d})$ (NE monsoon). The opposite trend also was found in Z1, where variability varied from $2\,696\text{ mg}/(\text{m}^2\cdot\text{d})$ (NE monsoon) to $1\,500\text{ mg}/(\text{m}^2\cdot\text{d})$ (pre-monsoon). Similar variability was observed in both Z3 and Z5. For example, pre-monsoon shows higher, and NE-monsoon shows lower. However, compared to Z1–Z3 and Z5, Z4 did not show more significant variability (Table 1).

3.2 Monthly and seasonal distribution and variability of SSS

Monthly SSS largely varied from Z1 to Z5. SSS in Z1 changes between 32.4 to 22.6 with an average of 28.6. For Z2, SSS is the

most variable (28.9–16.8) across the month, where lower (~ 17.5) from July to October and higher (28–30) from January to May. In Z3, SSS changes between 26.3 to 33.01, where early January to August showed higher SSS. Similar trends were observed in Z4. Monthly SSS changes between 27.4 to 32 whereas January to August showed around 30, which is a relatively higher level (Fig. 7).

SSS of the BoB varied spatially, largely from north to south as well as seasonally, given the monsoon-dominated rainfall pattern and freshwater influxes from rivers. Overall, the SSS of the five zones fluctuated during SW and NE monsoon seasons, while it did not vary significantly during pre-monsoon (Fig. 8). Five zones display varying trends in seasonal salinity distribution, with Z1, Z2, and Z5 showing the highest variability during SW and NE monsoons, whereas Z3 experienced frequent fluctuations in variation trends during the same seasons (Table 2, Fig. 7). As stated earlier, a network of small to medium-sized rivers drains into Z1, and its SSS variability changes vastly during SW and NE monsoons, but there is no significant variability of SSS during pre-monsoon due to the inactive monsoon mode.

Seasonal averaged SSS ranged from 19 to 32. Z1–Z2 is located

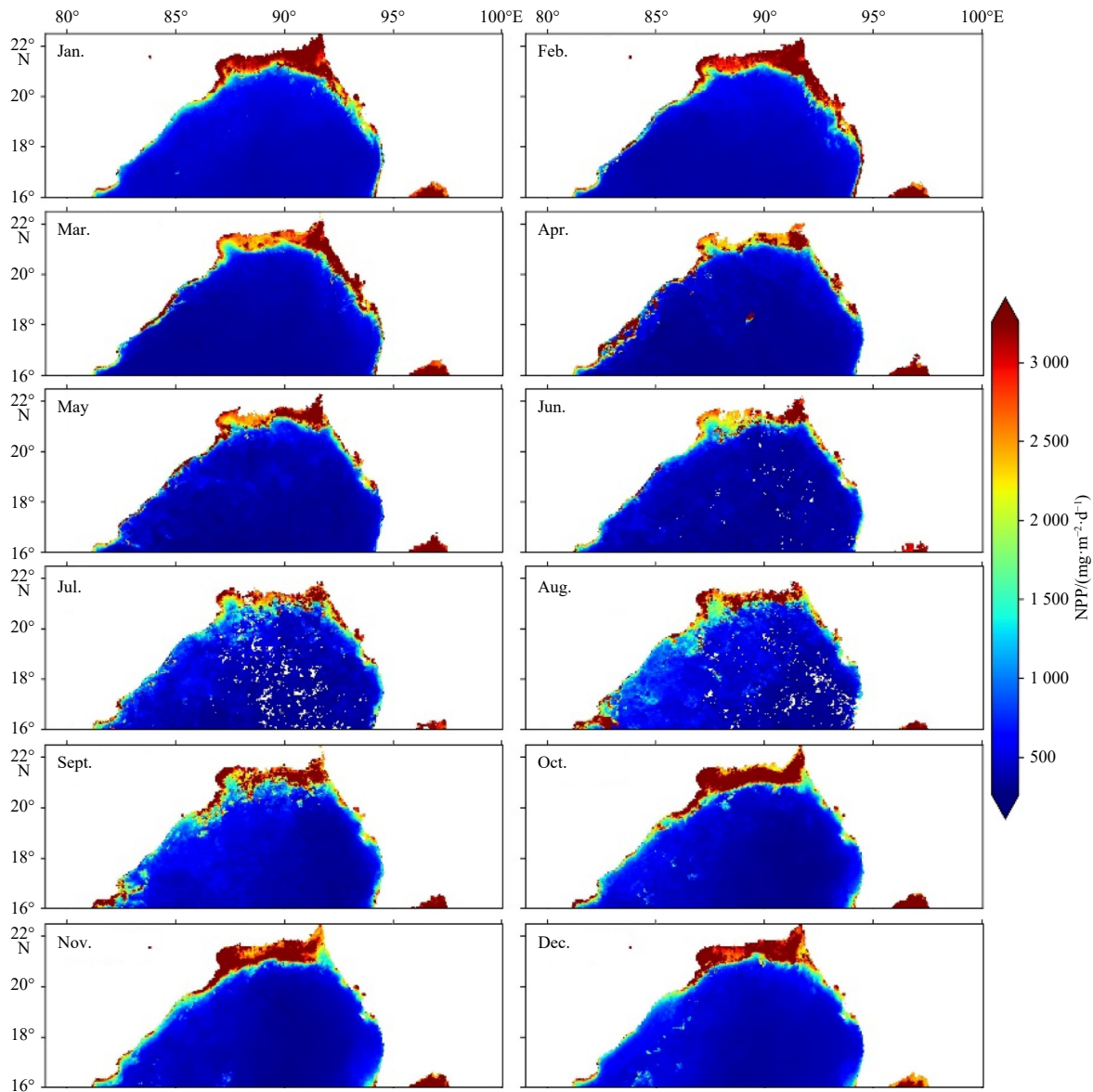


Fig. 4. Monthly net primary productivity (NPP, in terms of C) maps in the northern Bay of Bengal.

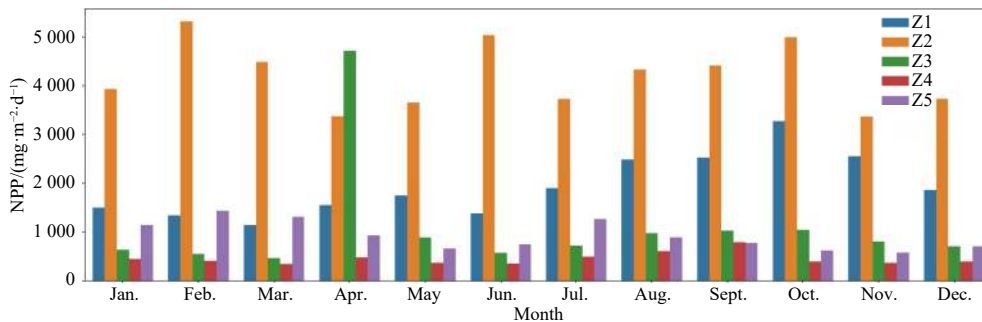


Fig. 5. Monthly net primary productivity (NPP, in terms of C) distribution.

close to the Ganges, Brahmaputra, Meghna (GBM) river system, which is why salinity is low relative to the other zones. Seasonally, SSS ranged from 32.1 to 25.8 in Z1, but it varied from 19.8 to 32, in which Z2 received huge freshwater river discharge and rainfall during SW monsoon, which is probably the reason why SSS dropped around 19 in Z2. There is no significant salinity drop

in Z3 and Z4; instead, all seasons show higher SSS (Fig. 8, Table 2).

The maximum SSS variability for Z1 was 2.27 during NE monsoon, whereas the minimum was 0.48 during pre-monsoon. SSS for Z2 depends on freshwater discharge from the Meghna, Padma, and Ganges-Brahmaputra rivers. The maximum SSS variability for Z2 was 6.67 during SW monsoon, whereas the min-

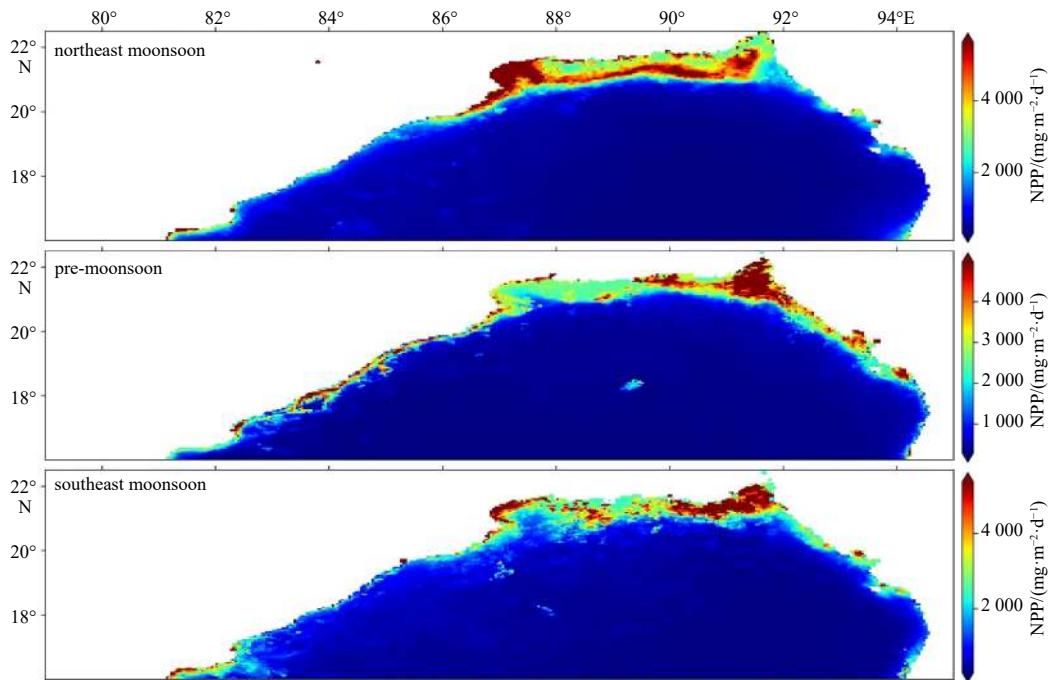


Fig. 6. Seasonal net primary productivity (NPP, in terms of C) maps in the northern Bay of Bengal.

Table 1. Seasonal NPP average and variability

Zone	NPP average (in terms of C)/(mg·m ⁻² ·d ⁻¹)			NPP variability (in terms of C)/(mg·m ⁻² ·d ⁻¹)		
	Northeast monsoon	Pre-monsoon	Southwest monsoon	Northeast monsoon	Pre-monsoon	Southwest monsoon
Z1	2 566.30	1 484.98	2 074.39	2 696.37	1 500.52	1 637.74
Z2	4 033.14	3 844.31	4 379.77	1 582.55	4 049.19	3 523.57
Z3	854.64	2 022.13	827.24	694.11	1 037.27	1 129.52
Z4	388.73	400.02	563.99	64.87	134.33	184.57
Z5	634.32	969.46	919.49	612.74	1 259.97	770.60

imum was 3.89 during pre-monsoon. Z3 also received river influx, which varied with seasons. This zone didn't experience considerable variability in SSS during SW and NE monsoons. The maximum SSS variability for Z3 was 1.02 during SW monsoon, whereas the minimum was 0.03 during pre-monsoon. Z4 is relatively deeper and away from any kind of coastal influence. It also experienced variations ranging from 0.2 to 1.0, where SSS variability ranged from 0.5 to 1.1, as well as in Z5 (Table 2).

3.3 Monthly and seasonal distribution and variability of SST

Monthly SST doesn't change significantly; however, the highest SST always remains around 30°C across all zones. In Z1, SST changes from 30°C to 23.9°C, averaging 28.03°C. Higher SST was found during the winter months, and higher SST was observed from April to October across the whole northern BoB. SST changes between 30°C and 22.9°C in Z2. Again, it has the same monthly distribution as Z2. Z3 to Z5 has a mean SST of 28°C and a range of 25°C to 30°C. During winter months, lower SST was observed near the coast, whereas the opposite was observed during warm months (Figs 9 and 10).

Seasonally, SST distribution varied from 27°C to 29°C. Every zone experiences an almost similar range of average change. For example, SST variability ranges from 0.51°C to 0.34°C across three seasons where SSTs were 27.6°C, 28.7°C, and 29.7°C in NE, pre-, and SW monsoons. The remaining three zones also show a change near 2°C. However, variability was highest in Z2 and Z5 during pre-monsoon, which is ~1.0 (Fig. 11, Table 3).

3.4 Monthly variability of euphotic zone depth

The computed EZD of northern BoB ranged between 6 m and 154 m (Fig. 12). Coastal Z1 and Z2 had lower EZDs than the deep ocean zones Z3–Z5. As EZD and NPP are negatively correlated, the beginning of the summer monsoon is marked by lower NPP, thus higher EZD for Z1, and the opposite, i.e., lower EZDs during the winter monsoon because of higher NPP, though Z1 was highly productive for the whole year.

As discussed before, Z2 is the most productive zone of northern BoB. Hence, the EZD was the shallowest in Z2 during the two monsoon seasons due to the influence of nutrient discharge from the GBM river systems. Z3 and Z5 are also partly influenced by the coastal waters; they are moderately productive during winter monsoon and have an EZD of 58 m to 103 m. Among the northern BoB zones, Z4 has the highest EZD value and is the least productive. There is no notable influence of monsoon on the NPP concentration at Z4. However, during the summer monsoon, Z4 shows a higher value of EZD and is the opposite during the winter monsoon.

3.5 Inter-annual variability and distribution of MLD, NPP, SSS, and SST

The study examined the decadal changes in the mix layer depth (MLD in meters) for five different zones from 1997 to 2017. Results indicated that for Z1, the MLD increased from 21.53 m in 1997 to 22.54 m in 2007, representing a decadal change of 1.003 m. However, the mix only slightly increased to 22.80 m in 2017, res-

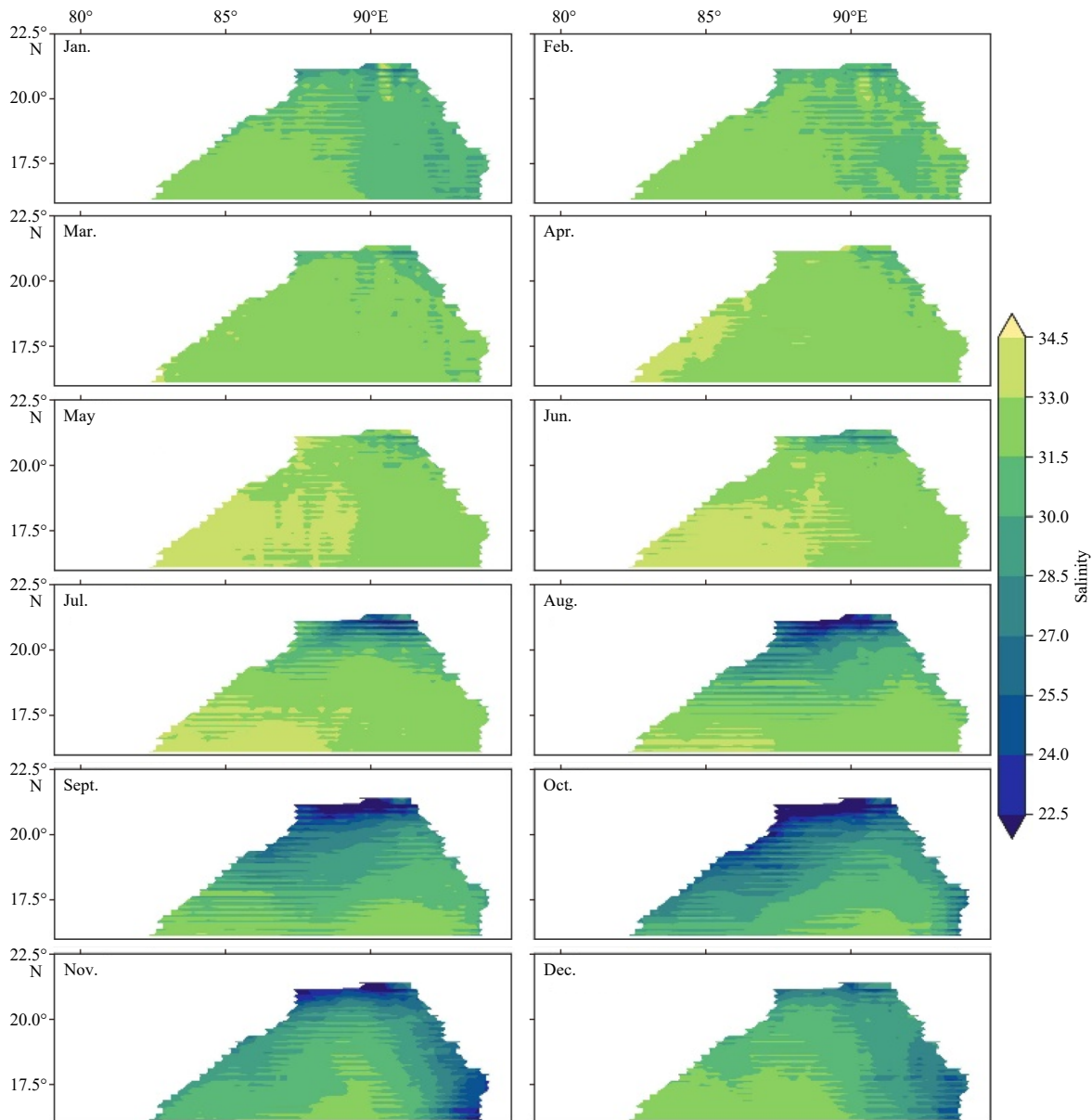


Fig. 7. Monthly-averaged sea surface salinity maps in the northern Bay of Bengal.

ulting in a smaller decadal change of 0.263 m. For Z2, the mix increased from 22.08 m in 1997 to 23.29 m in 2007, indicating a decadal change of 1.210 m. The mix continued to increase to 24.37 m in 2017, with a larger decadal change of 1.079 m. In Z3, the mix increased from 23.42 m in 1997 to 24.29 m in 2007, indicating a decadal change of 0.880 m. However, the mix decreased to 23.032 m in 2017, resulting in a negative decadal change of -1.265 m. For Z4, the mix increased from 28.56 m in 1997 to 30.25 m in 2007, indicating a decadal change of 1.688 m. Nevertheless, the mix slightly decreased to 30.09 m in 2017, resulting in a small negative decadal change of -0.154 m. Finally, for Z5, the mix increased from 22.85 m in 1997 to 24.44 m in 2007, indicating a decadal change of 1.592 m. The mix continued to increase to 25.23 m in 2017, with a smaller decadal change of 0.783 m. These findings highlight the varying rates of change in MLD across different zones and over time.

At Z1, NPP also had irregular distribution. In most cases, the range of values was different, e.g., September to October of several years (2010, 2009, and 2011, etc.) showed higher concentra-

tion. A significant interannual variation in NPP was observed in Z2 from 2005 to 2020. Moderate variation was also observed in Z1. The other zones, Z3 to Z5, did not have significant variations. From 2010 to 2020, NPP decreased from $952.5 \text{ mg}/(\text{m}^2\cdot\text{d})$ to $-59.7 \text{ mg}/(\text{m}^2\cdot\text{d})$ (negative values indicate decrease) across the zone in which Z4 showed a significant decrease ($-59.7 \text{ mg}/(\text{m}^2\cdot\text{d})$). However, other zones experienced more moderate to lower positive changes, such as $214.1 \text{ mg}/(\text{m}^2\cdot\text{d})$, $952.5 \text{ mg}/(\text{m}^2\cdot\text{d})$, $29.7 \text{ mg}/(\text{m}^2\cdot\text{d})$, and $558.0 \text{ mg}/(\text{m}^2\cdot\text{d})$.

Over the years from 2010 to 2020, Z1, Z3–Z5 have shown consistent salinity in the range of 30 to 32. Between 2015 and 2017, the salinity level dropped rapidly (27.2 to 19.1) in Z2. This is probably attributed to the increase in freshwater inputs and an unusual rainfall pattern. SSS's decadal change (2010–2020) varied from 1.05 to -4.42 across the zones. The most positive change (1.05) was found in Z3, whereas the negative (-4.42) was found in Z2.

Our monthly SST data did not capture a significant variation across all zones, but it is interesting to note that significant vari-

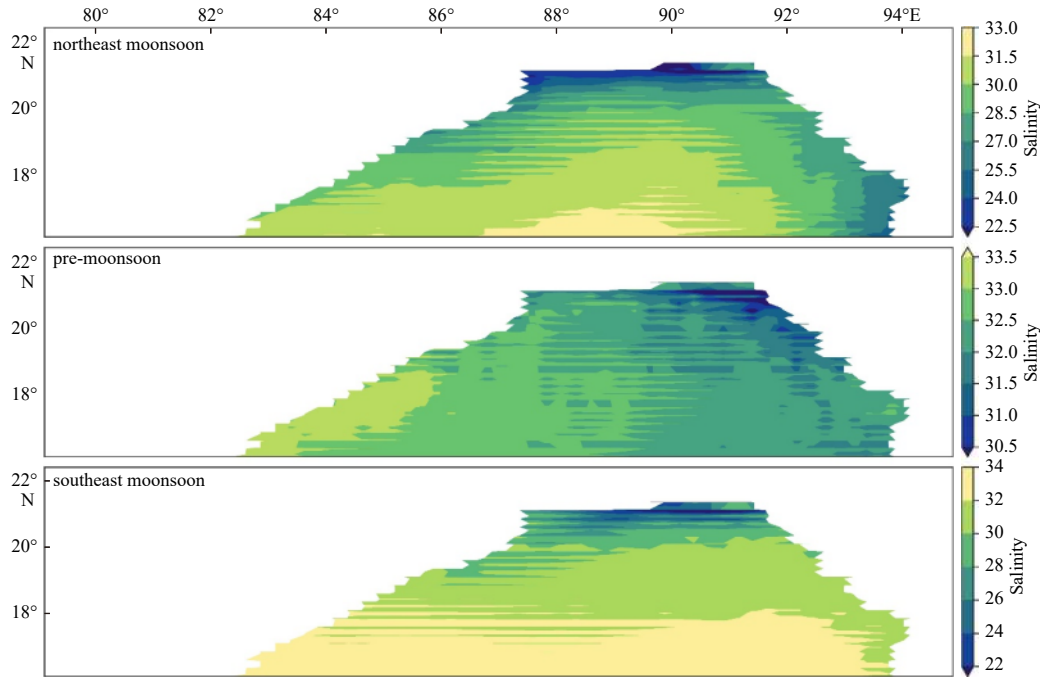


Fig. 8. Seasonal average sea surface salinity maps in the northern Bay of Bengal.

Table 2. Seasonal sea surface salinity (SSS) average and variability

Zone	SSS average			SSS variability		
	Northeast monsoon	Pre-monsoon	Southwest monsoon	Northeast monsoon	Pre-monsoon	Southwest monsoon
Z1	25.842	32.144	27.024	2.279	0.480	2.670
Z2	20.710	32.144	19.807	4.820	3.899	6.671
Z3	28.779	32.144	30.856	0.987	0.332	1.020
Z4	30.214	32.144	31.258	1.073	0.282	0.976
Z5	28.211	32.144	30.786	1.096	0.529	1.280

ations across all zones in the northern BoB were observed inter-annually. Z3–Z5 have the most similar sea surface temperature distributions, and Z1 to Z2 have similar distributions as well. The decadal change (2010–2020) of SST ranged from 0.56 °C to 0.19 °C, in which Z4 showed more positive change (0.56 °C). Other zones experienced moderate to lower positive change, e.g., 0.31 °C, 0.19 °C, 0.37 °C, 0.56 °C, and 0.27 °C were found from Z1 to Z5, respectively (Fig. 13).

3.6 The relationship analysis among NPP, MLD, SST, and EZD

The correlation analysis between NPP and MLD revealed an overall Pearson Correlation Coefficient (PCC) of 0.23 ($p = 0.003$), which indicates a positive correlation between NPP and MLD. The PCC for each of the five zones were as follows: -0.3 for Z1, 0 for Z2, -0.3 for Z3, -0.1 for Z4, and 0.4 for Z5 (Fig. 14).

No significant correlation was observed between SST and NPP distribution in the northern BoB (Fig. 12). PCC between SST and NPP for Z1 was 0.2 ; for Z2, it was 0.0 ; for Z3, it was 0.1 ; for Z4, it was 0.0 ; and for Z5, it was -0.2 . A similar figure was also found between NPP and SSS (Figs 15, S1).

The NPP is negatively (≥ -0.4) correlated with euphotic depth in every zone (Fig. 16). PCC between NPP and EDZ for Z1 was -0.5 ; for Z2, it was -0.2 ; for Z3, it was -0.5 ; for Z4, it was -0.4 ; and for Z5, it was -0.5 .

We did not find any association between NPP, SST, and SSS in our study areas. EZD correlates with NPP because the ocean's remote sensing NPP was originally derived from a vertically gener-

alized production model (VGPM) (Behrenfeld and Falkowski, 1997), which incorporates euphotic depth and absorption coefficient of phytoplankton over 400–700 nm just below the sea surface.

4 Discussion

Monthly, seasonal, and interannual spatio-temporal distribution of NPP, MLD, SST, SSS, and EZD have been analyzed for the northern BoB using five sub-grids. NPP spatio-temporal changes are caused by variations in phytoplankton biomass and environmental factors such as light penetration, nutrients, salinity, temperature, and surface turbulence, as indicated by SST, SSS, and EZD (George et al., 2013; Kong et al., 2019). The BoB is located within the tropics, and nutrient discharge from the rivers and estuaries dominates its seasonal cycle of primary productivity, in addition to a seasonally changing wind system. The availability of light and nutrients generally control the primary productivity in BoB; in addition, seasonally reversing monsoonal wind, freshwater input, and remote atmospheric forcing, the IOD profoundly affects the productivity in the BoB. The seasonal reversal in distribution of NPP, especially at Z2 and Z1, is happening because of these biophysical processes. Upwelling processes in the BoB only occur close to the coast within 40 km (Shetye et al., 1991). Seasonally reversing monsoonal wind forcing facilitates mixing of highly stratified northern BoB, which brings nutrients to the photic zone. For the northernmost Z1 and Z2, a continuous supply of nutrients from the major Ganges-Brahmaputra-Meghna

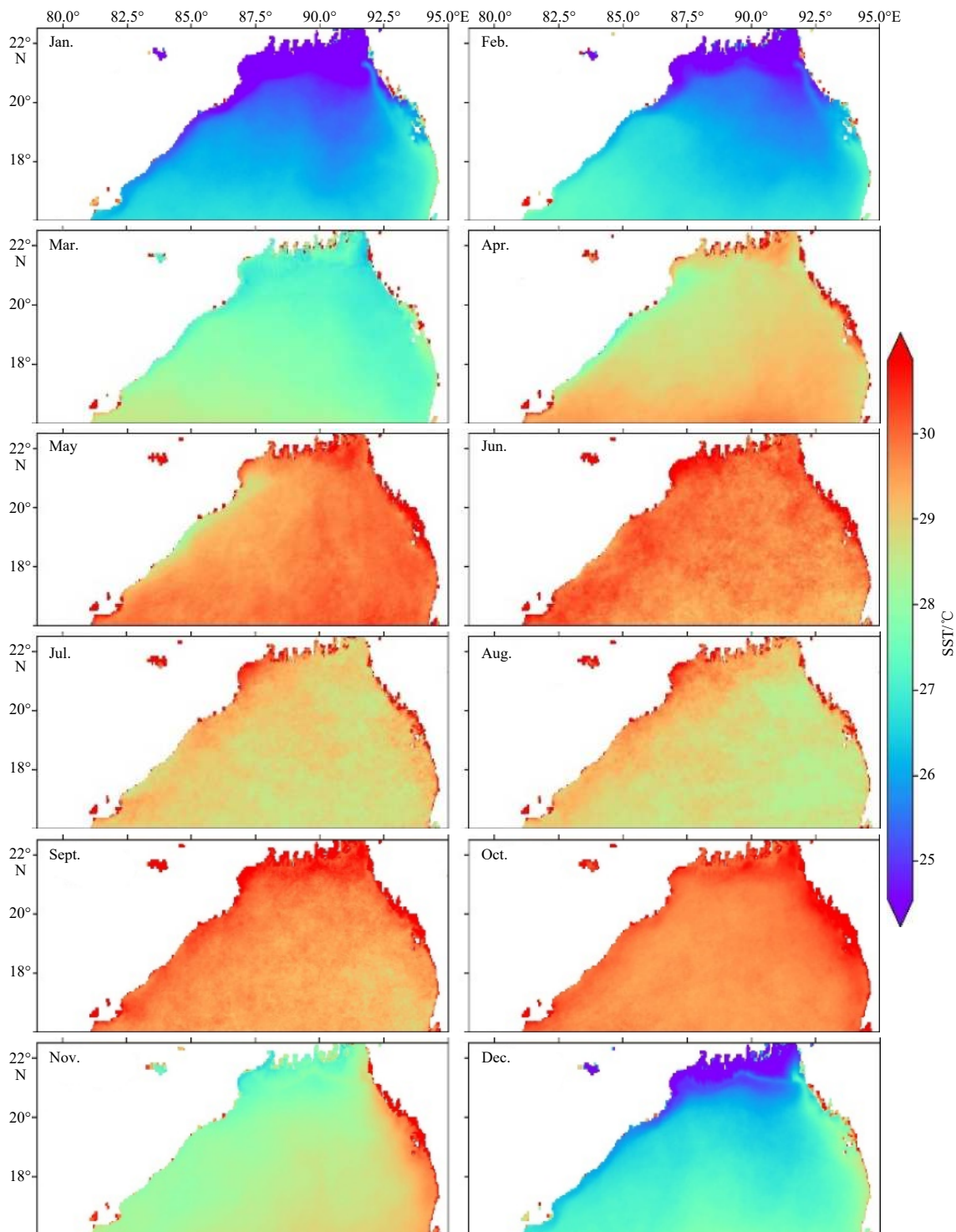


Fig. 9. Monthly-averaged sea surface temperature (SST) maps.

river system and subsequent mixing promotes primary productivity, which was observed consistently in our study.

The circulation dynamics of Z3 is dominated by the East Indian Coastal Current (EICC), which flows equatorward from August to December and poleward (northeast) from February to May (Chaitanya et al., 2015; Shetye et al., 1996). This zone experiences strong seasonal upwelling and efficient mixing due to the reversal of monsoonal winds and shelf bathymetric features. During the SW monsoon, the east coast of India experiences favorable winds for upwelling (Shetye et al., 1991). At the same

time, EICC affects Chl *a* distribution in Z3 by affecting nutrient transport, light penetration, and temperature in the euphotic zone (Shanthi et al., 2015). During the SW monsoon, our analysis showed the highest level (900.90 mg/(m²·d)) of NPP in Z3, which falls under the east coast of India. Productivity is probably driven by the monsoon season with shallower thermoclines, more vigorous vertical mixing, less rain (Currie et al., 2013; Wiggert et al., 2009). Some studies (Behrenfeld, 2014; Sarker et al., 2020; Sarker and Wiltshire, 2017) reported a declining trend of primary productivity across the BoB. However, our long-term data showed a

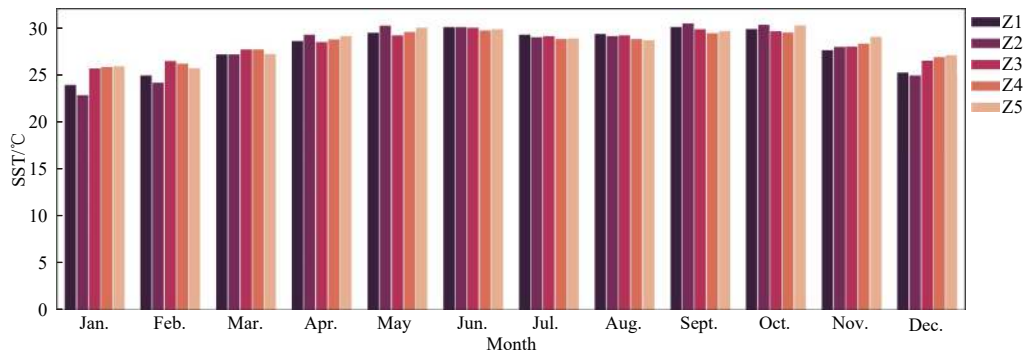


Fig. 10. Monthly averaged sea surface temperature distribution from the five zones.

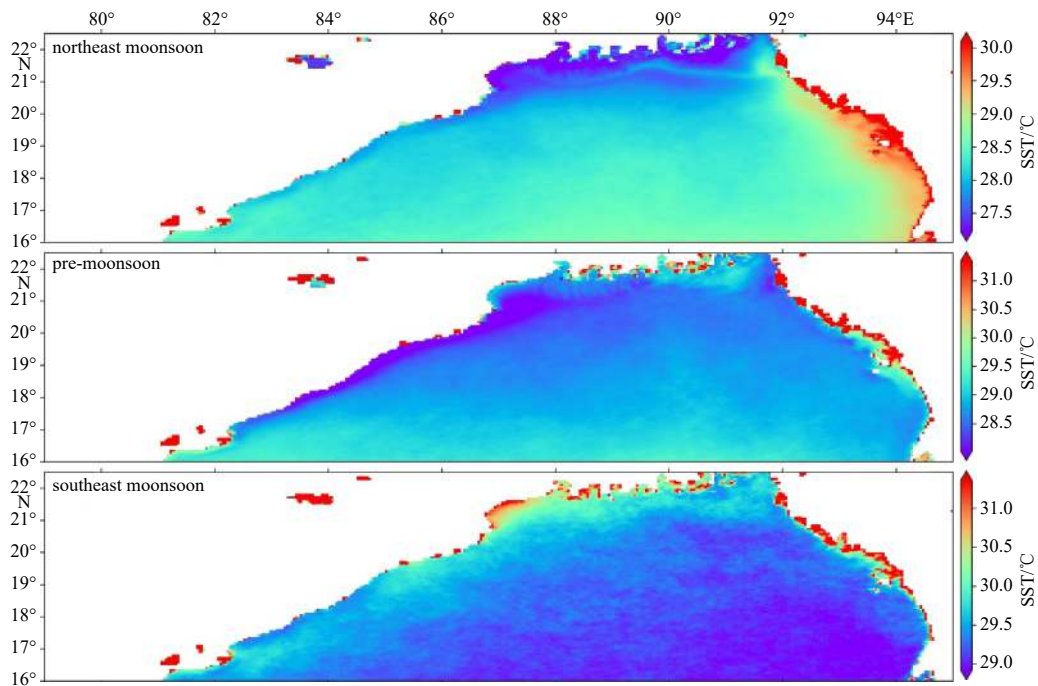


Fig. 11. Seasonal sea surface temperature (SST) distribution.

Table 3. Seasonal sea surface temperature (SST) average and variability

Zone	SST average/°C			SST variability/°C		
	Northeast monsoon	Pre-monsoon	Southwest monsoon	Northeast monsoon	Pre-monsoon	Southwest monsoon
Z1	27.65	28.47	29.761 97	0.339	0.581	0.513
Z2	27.81	28.95	29.727 03	0.660	1.025	0.593
Z3	28.10	28.52	29.597 49	0.216	0.643	0.374
Z4	28.28	28.72	29.247 56	0.130	0.147	0.102
Z5	28.87	28.84	29.319 5	0.868	1.218	0.678

perceptible decline in Z4 only. Our finding showed that decadal change in NPP varied from 952.5 mg/(m²·d) to -59.7 mg/(m²·d). Overall, four coastal zones (Z1–Z3 and Z5) experienced positive change, which means an increase in productivity, whereas negative change, meaning reduced productivity, was found in Z4. A slightly lower increase was found in Z5 because it does not receive a considerable amount of freshwater input like Z2, and the effect of seasonally reversing wind is less pronounced. Z4 is an open ocean environment and is far away from the influence of coastal turbid water and experiences poor vertical mixing. It is also the lowest productive zone, and Fig. 16 shows the increasing trend of SST in this zone. Chaitanya et al. (2015) found that Chl *a*

concentration in the open ocean was low, between 0.06 mg/m³ and 5.5 mg/m³. Productivity in the open ocean is generally low due to strong stratification associated with barrier layers, which prevents the exchange of nutrients from deep water to surface water. The occasional passage of tropical cyclones over Z4 helps to break the strong stratification and thereby inject nutrients into the photic zone that enhances productivity. However, several studies have reported an expanding dead zone in the middle of the BoB, and decadal reduced, lower productivity and warmer water indicate stratification and reduction of mixing depth, hence an intense oxygen minimum zone in Z4 (Diaz and Rosenberg, 2008; Sridevi and Sarma, 2020). The results of our study in-

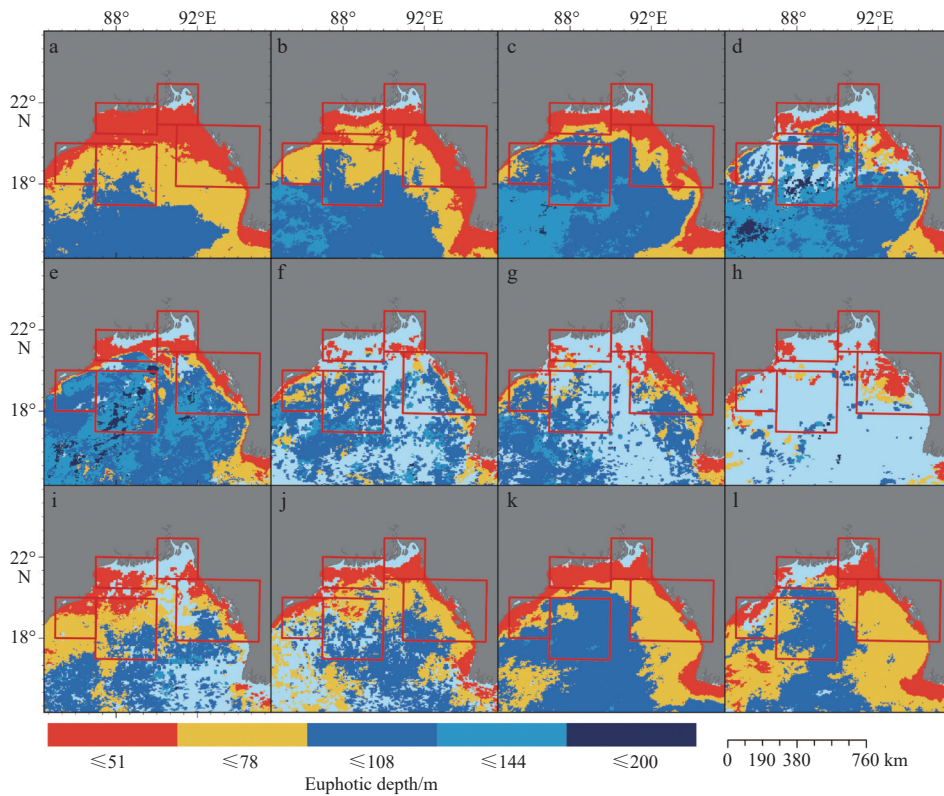


Fig. 12. Monthly distribution of euphotic depth. a–l presents months from January to December.

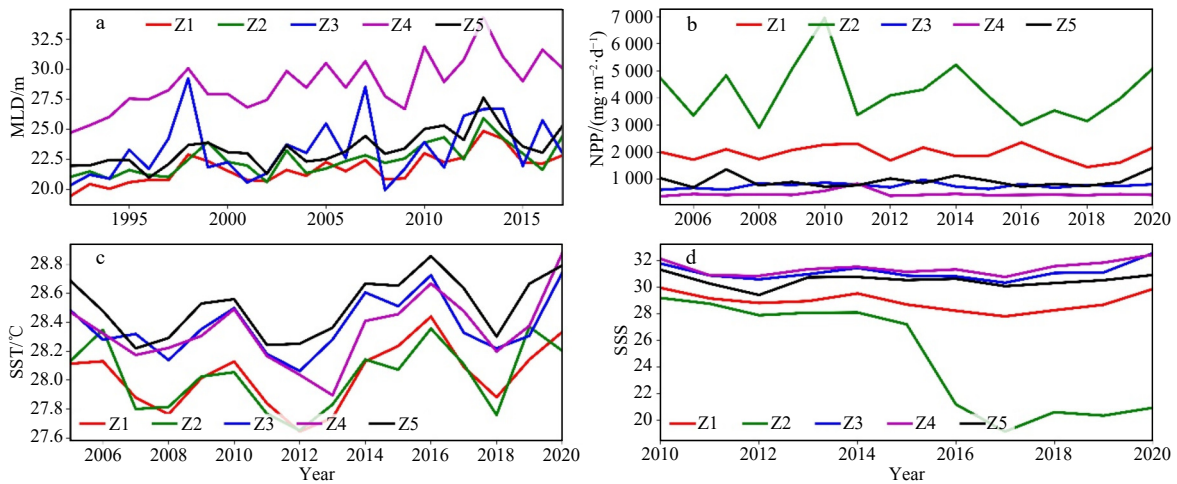


Fig. 13. Inter-annual distribution of mixed layer depth (MLD) (a), net primary productivity (NPP, in terms of C) (b), sea surface temperature (SST) (c), and sea surface salinity (SSS) (d).

dicates that the MLD in Z3 and Z4 exhibited a decreasing trend over the two-decade period with a negative correlation with the NPP. This finding suggests that the water column in these zones may be becoming less mixed over time. Such a decrease in mixing could potentially have significant implications for the biological productivity of the area. A less mixed water column can result in less nutrient cycling and lower levels of primary productivity, which could ultimately impact higher trophic levels in the ecosystem. However, our findings reveal that opposite scenarios occurred in Z1, Z2 and Z5. Across Z1–Z5, the NPP ranges from 5 315 mg/(m²·d) to 346.7 mg/(m²·d). Seasonally, NPP varied significantly. According to our findings, NPP distribution in Z2 is highest during SE monsoon, while it is higher in Z1 during NE

monsoon. Despite being close to each other, these are completely opposite scenarios. The BoB is also exposed to powerful tropical cyclones from October to December. From 2005 to 2020, about fifteen major cyclones traversed across the BoB, and these months (October and November) exhibit the most productivity on the eastern Indian coast and adjoining open sea due to cyclone-induced upwelling and vertical mixing, which favors higher productivity (Latha et al., 2015). Several studies found that seasonal and inter-annual variability in SSS is highest close to the northern part and minimum in the central zones (Akhil et al., 2014; Chaitanya et al., 2015). In the northern BoB, especially Z1–Z3 and Z5, the SSS varies with the amount of river fluxes. The SSS exhibits the greatest variability at Z1 (32.4–22.6) and fol-

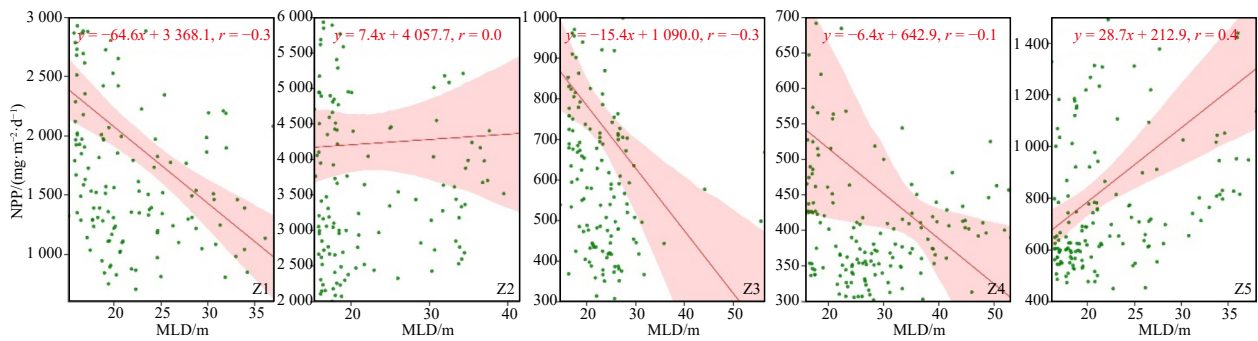


Fig. 14. Correlation between net primary productivity (NPP, in terms of C) and mixed layer depth (MLD).

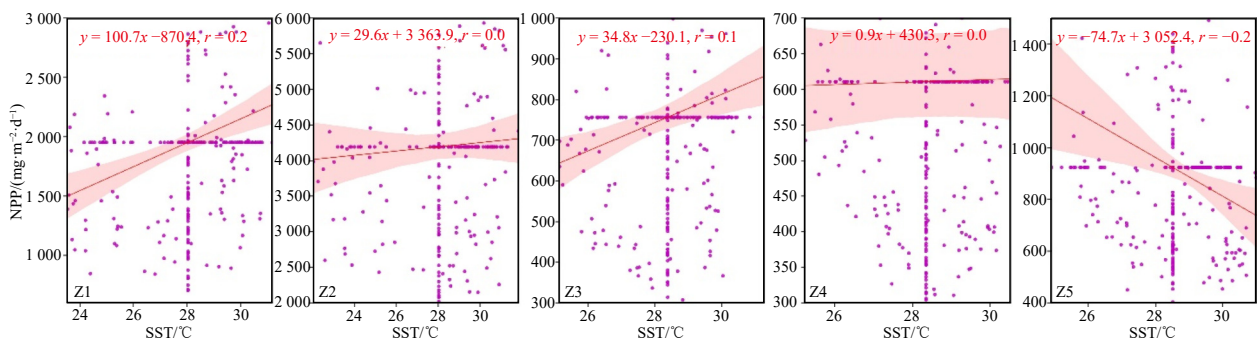


Fig. 15. Correlation between sea surface temperature (SST) and net primary productivity (NPP, in terms of C) in five different zones.

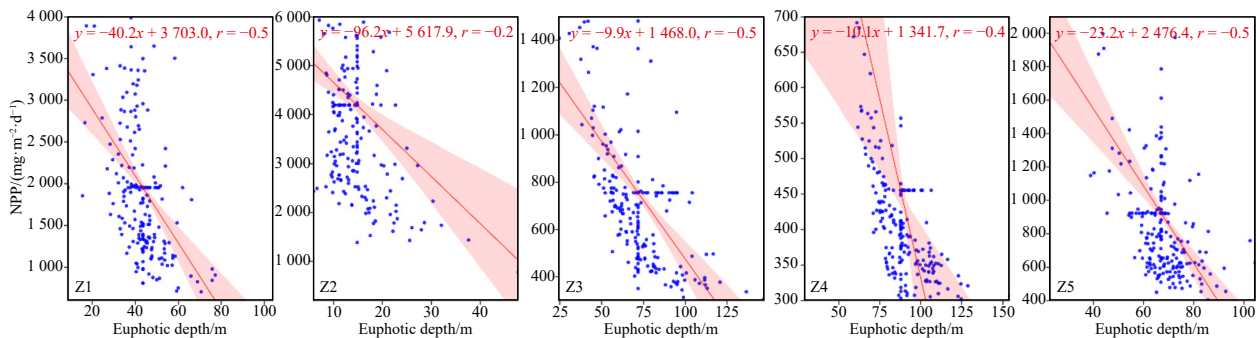


Fig. 16. Correlation between net primary productivity (NPP, in terms of C) and euphotic depth.

lowed by Z2 (28.9–16.8), over the course of the study. This is due to the fact that they are mostly located at the mouth of major rivers. Z2 and Z1 showed the highest variability during SW and NE monsoons, whereas Z3 experienced frequent fluctuations in variation trends during the same seasons. In Z1, SSS varied from 3.89 to 6.67 during the SW monsoon, with 6.67 found during the SW monsoon. The lowest variations (1.0 to 0.2) and highest SSS confidence (~32 to 30) were found in Z4 because this is far from the coast and river influence. SSS's decadal change (2010–2020) varied from 1.05 to -4.42 across the zones. The negative values observed from Z2 indicate salinity decreasing over time due to higher freshwater inputs and rainfall from an intense monsoon season. This can also be caused by more Himalayan ice melting due to global warming. Although changes in SST are associated with changes in Chl *a*, NPP, species physiological response, and distribution (Behrenfeld et al., 2006; Dunstan et al., 2018), *r* values between calculated monthly SST and NPP are low (0 to 0.2) from Z1 to Z4, whereas a negative *r* value has been found in Z5. However, the decadal change (2010–2020) of SST ranged from 0.56°C to 0.19°C , which indicates SST is increasing over time.

These changes might be due to rapidly increasing atmospheric CO_2 concentration and climate changes (D'Mello & Prasanna Kumar, 2016; Levitus et al., 2001). Oceanic water mass dynamics are governed by temperature, which is a key indicator of climate change (Roemmich et al., 2012). Approximately 90% of the excess heat added to the earth's climate system since the 1960s is stored in the oceans (Levitus et al., 2001). Based on studies (Alory et al., 2007; Chambers et al., 1999; D'Mello & Prasanna Kumar, 2016; Dong et al., 2014), there has been an overall warming of the ocean over the past half-century. A significant increase in water temperature in the BoB is also supported by D'Mello and Prasanna Kumar (2016), who reported an increase in SST at a rate of 0.014°C per year in the BoB from 1960 to 2011.

5 Conclusions

Daily and monthly imagery and gridded data sets were analyzed to study the spatio-temporal variations in NPP, EZD, MLD, SST, and SSS in the northern BoB from January 2005 to August 2020, and the findings would contribute to a better understanding of tropical ocean ecology of a regional sea under long term

climate change scenarios. The BoB, as a regional northward extension of the Indian Ocean, does not experience large-scale seasonal and spatial variability in primary productivity and SST. However, seasonal variability in freshwater discharge from the rivers along the northern bay affects the SSS distribution significantly, particularly for the two northern zones, Z1 and Z2. Z2 is the most productive of the five zones that we have analyzed, and it is driven by a heavy influx of nutrients from the rivers and the mixing due to seasonally reversing monsoon winds. We also noticed that sea surface temperature and sea surface salinity do not correlate with the region's primary productivity, implying that other regional phenomena, viz., coastal upwelling, mixing from wind reversal, and passage of power cyclones, etc., played a significant role in the primary productivity. EZD is deeper during the summer monsoon while shallower during the wintertime, with a corresponding increase in productivity. The bay is highly stratified from the large influx of freshwater discharge from the Ganges, Brahmaputra, and Meghna rivers. Turbidity also plays a critical role in inhibiting primary productivity in the northern head bay region. The BoB is relatively less productive due to stratification and less efficient mixing or upwelling compared with the nearest Arabian Sea, with ephemerally elevated productivity. More research is needed to further understand the variations and impacts of localized processes on primary productivity.

Acknowledgements

The authors thank the US Embassy in Dhaka, Bangladesh, and the US Department of State for sponsoring undergraduate exchange program at Florida Gulf Coast University to carry out this research in Lab of Jose.

References

- Abdul-Hadi A, Mansor S, Pradhan B, et al. 2013. Seasonal variability of chlorophyll-*a* and oceanographic conditions in Sabah waters in relation to Asian monsoon—a remote sensing study. *Environmental Monitoring and Assessment*, 185(5): 3977–3991, doi: [10.1007/s10661-012-2843-2](https://doi.org/10.1007/s10661-012-2843-2)
- Akhil V P, Durand F, Lengaigne M, et al. 2014. A modeling study of the processes of surface salinity seasonal cycle in the Bay of Bengal. *Journal of Geophysical Research: Oceans*, 119(6): 3926–3947, doi: [10.1002/2013JC009632](https://doi.org/10.1002/2013JC009632)
- Alory G, Wijffels S, Meyers G. 2007. Observed temperature trends in the Indian Ocean over 1960–1999 and associated mechanisms. *Geophysical Research Letters*, 34(2): L02606
- Arthur M A, Zachos J C, Jones D S. 1987. Primary productivity and the Cretaceous/Tertiary boundary event in the oceans. *Cretaceous Research*, 8(1): 43–54, doi: [10.1016/0195-6671\(87\)90011-5](https://doi.org/10.1016/0195-6671(87)90011-5)
- Balch W, Evans R, Brown J, et al. 1992. The remote sensing of ocean primary productivity: use of a new data compilation to test satellite algorithms. *Journal of Geophysical Research: Oceans*, 97(C2): 2279–2293, doi: [10.1029/91JC02843](https://doi.org/10.1029/91JC02843)
- Behrenfeld M J. 2014. Climate-mediated dance of the plankton. *Nature Climate Change*, 4(10): 880–887, doi: [10.1038/nclimate2349](https://doi.org/10.1038/nclimate2349)
- Behrenfeld M J, Falkowski P G. 1997. Photosynthetic rates derived from satellite-based chlorophyll concentration. *Limnology and Oceanography*, 42(1): 1–20, doi: [10.4319/lo.1997.42.1.0001](https://doi.org/10.4319/lo.1997.42.1.0001)
- Behrenfeld M J, O'Malley R T, Siegel D A, et al. 2006. Climate-driven trends in contemporary ocean productivity. *Nature*, 444(7120): 752–755, doi: [10.1038/nature05317](https://doi.org/10.1038/nature05317)
- Bharathi M D, Sarma V V S S, Rameswari K, et al. 2018. Influence of river discharge on abundance and composition of phytoplankton in the western coastal Bay of Bengal during peak discharge period. *Marine Pollution Bulletin*, 133: 671–683, doi: [10.1016/j.marpolbul.2018.06.032](https://doi.org/10.1016/j.marpolbul.2018.06.032)
- Capuzzo E, Lynam C P, Barry J, et al. 2018. A decline in primary production in the North Sea over 25 years, associated with reductions in zooplankton abundance and fish stock recruitment. *Global Change Biology*, 24(1): e352–e364
- Chaitanya A V S, Durand F, Mathew S, et al. 2015. Observed year-to-year sea surface salinity variability in the Bay of Bengal during the 2009–2014 period. *Ocean Dynamics*, 65(2): 173–186, doi: [10.1007/s10236-014-0802-x](https://doi.org/10.1007/s10236-014-0802-x)
- Chambers D P, Tapley B D, Stewart R H. 1999. Anomalous warming in the Indian Ocean coincident with El Niño. *Journal of Geophysical Research: Oceans*, 104(C2): 3035–3047, doi: [10.1029/1998JC900085](https://doi.org/10.1029/1998JC900085)
- Currie J C, Lengaigne M, Vialard J, et al. 2013. Indian Ocean dipole and El Niño/Southern Oscillation impacts on regional chlorophyll anomalies in the Indian Ocean. *Biogeosciences*, 10(10): 6677–6698, doi: [10.5194/bg-10-6677-2013](https://doi.org/10.5194/bg-10-6677-2013)
- D'Mello J R, Prasanna Kumar S. 2016. Why is the Bay of Bengal experiencing a reduced rate of sea surface warming?. *International Journal of Climatology*, 36(3): 1539–1548
- Diaz R J, Rosenberg R. 2008. Spreading dead zones and consequences for marine ecosystems. *Science*, 321(5891): 926–929, doi: [10.1126/science.1156401](https://doi.org/10.1126/science.1156401)
- Dong Lu, Zhou Tianjun, Wu Bo. 2014. Indian Ocean warming during 1958–2004 simulated by a climate system model and its mechanism. *Climate Dynamics*, 42(1–2): 203–217, doi: [10.1007/s00382-013-1722-z](https://doi.org/10.1007/s00382-013-1722-z)
- Dunstan P K, Foster S D, King E, et al. 2018. Global patterns of change and variation in sea surface temperature and chlorophyll *a*. *Scientific Reports*, 8(1): 14624, doi: [10.1038/s41598-018-33057-y](https://doi.org/10.1038/s41598-018-33057-y)
- Frey K E, Comiso J C, Cooper L W, et al. 2017. Arctic Ocean primary productivity. Arctic Report Card 2017, NOAA. [http://www.Arctic.Noaa.Gov/Report-Card/Report-Card-2017/ArtMID/7798/ArticleID/701/Arctic-Ocean-Primary-Productivity\[2017-05-23/2022-07-08\]](http://www.Arctic.Noaa.Gov/Report-Card/Report-Card-2017/ArtMID/7798/ArticleID/701/Arctic-Ocean-Primary-Productivity[2017-05-23/2022-07-08])
- Frolov S, Ryan J P, Chavez F P. 2012. Predicting euphotic-depth-integrated chlorophyll-*a* from discrete-depth and satellite-observable chlorophyll-*a* off central California. *Journal of Geophysical Research: Oceans*, 117(C5): C05042
- George J V, Nuncio M, Chacko R, et al. 2013. Role of physical processes in chlorophyll distribution in the western tropical Indian Ocean. *Journal of Marine Systems*, 113–114: 1–12
- Gopalakrishna V V, Murty V S N, Sengupta D, et al. 2002. Upper ocean stratification and circulation in the northern Bay of Bengal during southwest monsoon of 1991. *Continental Shelf Research*, 22(5): 791–802, doi: [10.1016/S0278-4343\(01\)00084-X](https://doi.org/10.1016/S0278-4343(01)00084-X)
- Hendiarti N, Siegel H, Ohde T. 2004. Investigation of different coastal processes in Indonesian waters using SeaWiFS data. *Deep-Sea Research Part II: Topical Studies in Oceanography*, 51(1–3): 85–97, doi: [10.1016/j.dsr2.2003.10.003](https://doi.org/10.1016/j.dsr2.2003.10.003)
- Hossain M S, Sarker S, Sharifuzzaman S M, et al. 2020. Primary productivity connects hilsa fishery in the Bay of Bengal. *Scientific Reports*, 10(1): 5659, doi: [10.1038/s41598-020-62616-5](https://doi.org/10.1038/s41598-020-62616-5)
- Hoyer S, Hamman J. 2017. xarray: N-D labeled arrays and datasets in Python. *Journal of Open Research Software*, 5(1): 10, doi: [10.5334/jors.148](https://doi.org/10.5334/jors.148)
- Hussain M G, Hoq E. 2010. Sustainable Management of Fisheries Resources of the Bay of Bengal. Bangladesh: Support to Sustainable Management of the BOBLME Project
- Jaswal A K, Singh V, Bhambak S R. 2012. Relationship between sea surface temperature and surface air temperature over Arabian Sea, Bay of Bengal and Indian Ocean. *The Journal of Indian Geophysical Union*, 16(2): 41–53
- Kay S, Caesar J, Janes T. 2018. Marine dynamics and productivity in the Bay of Bengal. In: Nicholls R J, Hutton C W, Adger W N, et al, eds. *Ecosystem Services for Well-Being in Deltas*. Cham: Palgrave Macmillan
- Kong Fanping, Dong Qing, Xiang Kunsheng, et al. 2019. Spatiotemporal variability of remote sensing ocean net primary production and major forcing factors in the Tropical Eastern Indian and Western Pacific Ocean. *Remote Sensing*, 11(4): 391, doi: [10.3390/rs11040391](https://doi.org/10.3390/rs11040391)
- Latha T P, Rao K H, Nagamani P V, et al. 2015. Impact of cyclone

- PHAILIN on chlorophyll-*a* concentration and productivity in the Bay of Bengal. *International Journal of Geosciences*, 6(5): 473–480, doi: [10.4236/ijg.2015.65037](https://doi.org/10.4236/ijg.2015.65037)
- Levitus S, Antonov J I, Wang Julian, et al. 2001. Anthropogenic warming of Earth's climate system. *Science*, 292(5515): 267–270, doi: [10.1126/science.1058154](https://doi.org/10.1126/science.1058154)
- Mahesh R, Saravanakumar A, Thangaradjou T, et al. 2020. Seasonal and spatial variations of mesozooplankton energy transfer efficiency determined using remotely sensed SST and Chl-*a* in the Bay of Bengal. *Regional Studies in Marine Science*, 40: 101482, doi: [10.1016/j.rsma.2020.101482](https://doi.org/10.1016/j.rsma.2020.101482)
- Mohanty S S, Pramanik D S, Dash B P. 2014. Primary productivity of Bay of Bengal at Chandipur in Odisha, India. *International Journal of Scientific and Research Publications*, 4(10): 1–6
- Mutshinda C M, Finkel Z V, Irwin A J. 2013. Which environmental factors control phytoplankton populations?. A Bayesian variable selection approach. *Ecological Modelling*, 269: 1–8, doi: [10.1016/j.ecolmodel.2013.07.025](https://doi.org/10.1016/j.ecolmodel.2013.07.025)
- Narvekar J, Prasanna Kumar S. 2014. Mixed layer variability and chlorophyll *a* biomass in the Bay of Bengal. *Biogeosciences*, 11(14): 3819–3843, doi: [10.5194/bg-11-3819-2014](https://doi.org/10.5194/bg-11-3819-2014)
- Prakash K R, Pant V. 2020. On the wave-current interaction during the passage of a tropical cyclone in the Bay of Bengal. *Deep-Sea Research Part II: Topical Studies in Oceanography*, 172: 104658, doi: [10.1016/j.dsr2.2019.104658](https://doi.org/10.1016/j.dsr2.2019.104658)
- Pramanik S, Mandal S, Shee A, et al. 2019. Tidal circulation studies using regional model in the Bay of Bengal. In: Murali K, Sriram V, Samad A, et al, eds. *Proceedings of the Fourth International Conference in Ocean Engineering (ICOE2018)*. Singapore: Springer, 829–836
- Prasanna Kumar S, Muraleedharan P M, Prasad T G, et al. 2002. Why is the Bay of Bengal less productive during summer monsoon compared to the Arabian Sea?. *Geophysical Research Letters*, 29(24): 2235, doi: [10.1029/2002GL016013](https://doi.org/10.1029/2002GL016013)
- Rahman M H. 2007. *Legal Regime of Marine Environment in the Bay of Bengal Vol. 1*. New Delhi: Atlantic Publishers & Distributors (P) Ltd., 38–39
- Raymont J E G. 2014. *Plankton & productivity in the oceans: Volume 1: Phytoplankton*. 2nd ed. Vol. 1. New York: Elsevier, Pergamon Press Inc., Maxwell House, Fairview Park, Elmsford, 65–66
- Raymont J E G. 2014. *Plankton & Productivity in the Oceans. Volume 1: Phytoplankton*. Oxford: Pergamon Press
- Roemmich D, John Gould W, Gilson J. 2012. 135 years of global ocean warming between the *Challenger* expedition and the Argo Programme. *Nature Climate Change*, 2(6): 425–428, doi: [10.1038/nclimate1461](https://doi.org/10.1038/nclimate1461)
- Saikranthi K, Radhakrishna B, Thota N R, et al. 2019. Differences in the association of sea surface temperature—precipitating systems over the Bay of Bengal and the Arabian Sea during southwest monsoon season. *International Journal of Climatology*, 39(11): 4305–4312, doi: [10.1002/joc.6074](https://doi.org/10.1002/joc.6074)
- Sakalli A. 2017. Sea surface temperature change in the Mediterranean Sea under climate change: a linear model for simulation of the sea surface temperature up to 2100. *Applied Ecology and Environmental Research*, 15(1): 707–716, doi: [10.15666/aeer/1501_707716](https://doi.org/10.15666/aeer/1501_707716)
- Salgado-Hernanz P M, Racault M F, Font-Muñoz J S, et al. 2019. Trends in phytoplankton phenology in the Mediterranean Sea based on ocean-colour remote sensing. *Remote Sensing of Environment*, 221: 50–64, doi: [10.1016/j.rse.2018.10.036](https://doi.org/10.1016/j.rse.2018.10.036)
- Sandeep K K, Pant V. 2019. Riverine freshwater plume variability in the Bay of Bengal using wind sensitivity experiments. *Deep-Sea Research Part II: Topical Studies in Oceanography*, 168: 104649, doi: [10.1016/j.dsr2.2019.104649](https://doi.org/10.1016/j.dsr2.2019.104649)
- Sarker S, Panassa E, Hossain M S, et al. 2020. A bio-physicochemical perspective of the Bay of Bengal. *Journal of the Marine Biological Association of the United Kingdom*, 100(4): 517–528, doi: [10.1017/S0025315420000442](https://doi.org/10.1017/S0025315420000442)
- Sarker S, Wiltshire K H. 2017. Phytoplankton carrying capacity: is this a viable concept for coastal seas?. *Ocean & Coastal Management*, 148: 1–8, doi: [10.1016/j.ocecoaman.2017.07.015](https://doi.org/10.1016/j.ocecoaman.2017.07.015)
- Satpathy K K, Mohanty A K, Sahu G, et al. 2011. Spatio-temporal variation in physicochemical properties of coastal waters off Kalpakkam, southeast coast of India, during summer, pre-monsoon and post-monsoon period. *Environmental Monitoring and Assessment*, 180(1–4): 41–62, doi: [10.1007/s10661-010-1771-2](https://doi.org/10.1007/s10661-010-1771-2)
- Shamsuzzaman M, Islam M M, Tania N J, et al. 2017. Fisheries resources of Bangladesh: present status and future direction. *Aquaculture and Fisheries*, 2(4): 145–156, doi: [10.1016/j.aaf.2017.03.006](https://doi.org/10.1016/j.aaf.2017.03.006)
- Shanthi R, Poornima D, Raja K, et al. 2015. Inter-annual and seasonal variations in hydrological parameters and its implications on chlorophyll *a* distribution along the southwest coast of Bay of Bengal. *Acta Oceanologica Sinica*, 34(6): 94–100, doi: [10.1007/s13131-015-0689-5](https://doi.org/10.1007/s13131-015-0689-5)
- Shetye S R, Gouveia A D, Shankar D, et al. 1996. Hydrography and circulation in the western Bay of Bengal during the northeast monsoon. *Journal of Geophysical Research: Oceans*, 101(C6): 14011–14025, doi: [10.1029/95JC03307](https://doi.org/10.1029/95JC03307)
- Shetye S R, Shenoi S S C, Gouveia A D, et al. 1991. Wind-driven coastal upwelling along the western boundary of the Bay of Bengal during the southwest monsoon. *Continental Shelf Research*, 11(11): 1397–1408, doi: [10.1016/0278-4343\(91\)90042-5](https://doi.org/10.1016/0278-4343(91)90042-5)
- Sridevi B, Sarma V V S S. 2020. A revisit to the regulation of oxygen minimum zone in the Bay of Bengal. *Journal of Earth System Science*, 129(1): 107, doi: [10.1007/s12040-020-1376-2](https://doi.org/10.1007/s12040-020-1376-2)
- Thushara V, Vinayachandran P N. 2016. Formation of summer phytoplankton bloom in the northwestern Bay of Bengal in a coupled physical-ecosystem model. *Journal of Geophysical Research: Oceans*, 121(12): 8535–8550, doi: [10.1002/2016JC011987](https://doi.org/10.1002/2016JC011987)
- Vinayachandran P N, Kurian J. 2007. Hydrographic observations and model simulation of the Bay of Bengal freshwater plume. *Deep-Sea Research Part I: Oceanographic Research Papers*, 54(4): 471–486, doi: [10.1016/j.dsr.2007.01.007](https://doi.org/10.1016/j.dsr.2007.01.007)
- Wiggert J D, Vialard J, Behrenfeld M J. 2009. Basin-wide modification of dynamical and biogeochemical processes by the positive phase of the Indian Ocean Dipole during the SeaWiFS era. In: Wiggert J D, Hood R R, Naqvi S W A, et al, eds. *Indian Ocean Biogeochemical Processes and Ecological Variability*. Washington: American Geophysical Union
- Zhou Xinquan, Duchamp-Alphonse S, Kageyama M, et al. 2020. Dynamics of primary productivity in the northeastern Bay of Bengal over the last 26 000 years. *Climate of the Past*, 16(5): 1969–1986, doi: [10.5194/cp-16-1969-2020](https://doi.org/10.5194/cp-16-1969-2020)

Supplementary information:

Fig. S1. Correlation between net primary productivity and sea surface salinity for the five different zones.

The supplementary information is available online at <https://doi.org/10.1007/s13131-023-2254-y> and <http://www.aosocean.com/>. The supplementary information is published as submitted, without typesetting or editing. The responsibility for scientific accuracy and content remains entirely with the authors.